J/ψ and Drell-Yan cross-sections in Pb-Pb interactions at 158 GeV/c per nucleon

M C. Abreu, B. Alessandro, C. Alexa, J. Astruc, C. Baglin, A. Baldit, M.
Bedjidian, F. Bellaiche, S. Beole, V. Boldea, et al.

J/ψ and Drell-Yan cross-sections in Pb-Pb interactions at 158 GeV/c per nucleon

NA50 Collaboration

M.C. ABREU[6a], B. ALESSANDRO[11b], C. ALEXA[2], J. ASTRUC[8], C. BAGLIN[1], A. BALDIT[4], M. BEDJIDIAN[12], F. BELLAICHE[12], S. BEOLÈ[11b], V. BOLDEA[2], G. BONAZZOLA[11b], P. BORDALO[6h], A. BORHANI[9], A. BUSSIÈRE[1], V. CAPONY[1], J. CASTOR[4], T. CHAMBON[4], B. CHAURAND[9], I. CHEVROT[4], B. CHEYNIS[12], E. CHIAVASSA[11b], C. CICALÓ[3], S. CONSTANTINESCU[2], J. CRUZ[6], W. DABROWSKI[11b], A. DE FALCO[3], G. DELLACASA[11d], N. DE MARCO[11b], A. DEVAUX[4], S. DITA[2], O. DRAPIER[12], B. ESPAGNON[4], J. FARGEIX[4], F. FLEURET[9], P. FORCE[4], M. GALLIO[11b], L. GATIGNON[5], Y.K. GAVRILOV[7], C. GERSCHEL[8], P. GIUBELLINO[11b], M.B. GOLUBEVA[7], M. GONIN[9], P. GORODETZKY[10], J.Y. GROSSIORD[12], P. GUAITA[11b,e], F.F. GUBER[7], A. GUICHARD[12], R. HAROUTUNIAN[12], M. IDZIK[11b], D. JOUAN[8], T.L. KARAVITCHEVA[7], L. KLUBERG[9], A.B. KUREPIN[7], G. LANDAUD[4], Y. LE BORNEC[8], C. LOURENÇO[5], L. LUQUIN[4], P. MACCIOTTA[3], A. MARZARI-CHIESA[11b], M. MASERA[11b], A. MASONI[3], S. MOURGUES[4], A. MUSSO[11b], F. OHLSSON-MALEK[12], P. PETIAU[9], A. PICCOTTI[11b], J.R. PIZZI[12], W.L. PRADO DA SILVA[11b,f], G. PUDDU[3], C. QUINTANS[6], C. RACCA[10], L. RAMELLO[11c], S. RAMOS[6h], P. RATO-MENDES[11b], L. RICCATI[11b], A. ROMANA[9], S. SARTORI[11], P. SATURNINI[4], E. SCOMPARIN[11b,g], S. SERCI[3], S. SILVA[6], C. SOAVE[11b], P. SONDEREGGER[5h], X. TARRAGO[8], P. TEMNIKOV[3], N.S. TOPILSKAYA[7], G. USAI[3], C. VALE[6], E. VERCELLIN[11b], and N. WILLIS[8].

[1] Laboratoire de Physique des Particules (LAPP), IN2P3-CNRS, Annecy-le-Vieux, France;
[2] Institute of Atomic Physics (IFA), Bucharest, Romania;
[3] Università di Cagliari/INFN, Cagliari, Italy;
[4] Laboratoire de Physique Corpusculaire, Université Blaise Pascal et IN2P3-CNRS, Clermont-Ferrand, France;
[5] CERN, Geneva, Switzerland;
[6] Laboratório de Instrumentação e Física Experimental de Partículas (LIP), Lisbon, Portugal;
[7] Institute for Nuclear Research (INR), Moscow, Russia;
[8] Institut de Physique Nucléaire, Université Paris-Sud et IN2P3-CNRS, Orsay, France;
[9] Laboratoire de Physique Nucléaire des Hautes Energies, Ecole Polytechnique et IN2P3-CNRS, Palaiseau, France;
[10] Centre de Recherches Nucléaires, Université Louis Pasteur et IN2P3-CNRS, Strasbourg, France;
[11] Università di Torino e INFN, Turin, Italy ;
[12] Institut de Physique Nucléaire de Lyon, Université Claude Bernard et IN2P3-CNRS , Villeurbanne, France.

[a] Also at FCUL, Universidade de Lisboa, Lisbon, Portugal; [b] Dipartimento di Fisica Sperimentale; [c] Dipartimento di Scienze e Tecnologie Avanzate; [d] II Facoltà di Scienze, Alessandria; [e] Now at Dipartimento di Fisica, Università di Padova, Padua, Italy; [f] Now at UERJ, Rio de Janeiro, Brazil; [g] Now at CERN, Geneva, Switzerland; [h] Also at IST, Universidade Técnica de Lisboa, Lisbon, Portugal.

ABSTRACT
First results are reported on J/ψ and Drell-Yan cross-sections in Pb-Pb reactions at 158 GeV/c per nucleon. The ratio of cross-sections $\sigma_{J/\psi} / \sigma_{DY}$ is studied as a function of the impact parameter of the collision estimated from the measured transverse energy.

1

1. Introduction

Starting in 1986, the formation of Quark Gluon Plasma in nucleus-nucleus interactions has been studied by the NA38 Collaboration [1], [2]. Among other potential signatures [3], charmonium and Drell-Yan production have been measured using incident proton, oxygen and sulfur beams. Experiment NA50 has been designed to extend this program to incident lead beams. This paper reports the results on J/ψ and Drell-Yan cross-sections in Pb-Pb reactions. The data were obtained at the CERN SPS, using a beam of ^{208}Pb nuclei at 158 GeV/c per nucleon incident momentum on a fixed Pb target.

2. Apparatus

The NA50 detector, schematically shown in figures 1 and 2 in its high mass set-up version, is an upgraded version of the NA38 apparatus. It is specifically designed to cope with the high radiation level, huge multiplicities and background induced by the incident Pb ions. It consists of a muon spectrometer with better high mass muon pair mass resolution than achieved in experiment NA38. It makes use of a segmented Pb target with vertex identification in order to precisely recognize the origin of the interaction and reject reinteractions of spectator fragments which could lead to incorrect measurements. Centrality can be estimated on an event by event basis using three independent detectors, an electromagnetic calorimeter, a multiplicity detector and a very forward hadronic calorimeter ("zero degree calorimeter").

2.1. The muon spectrometer

The muon spectrometer uses the same basic components as the spectrometer of experiment NA38 [2]. A toroidal air-gap magnet bends the tracks which are measured by eight three-plane multi-wire proportional chambers (PC1 to PC8). Four hodoscopes (R1 to R4) provide the muon

2

pair trigger. The trigger efficiency is measured with a new system of two hodoscopes (P1 and P2) especially designed and adapted for this purpose. With respect to experiment NA38, the muon spectrometer used in this experiment has been modified as follows:

- it covers the pseudo-rapidity interval $2.8 < \eta < 4.0$

- the current in the magnet is 7000 A, providing a pure toroidal field $B_\phi = 0.51$ T at a mean radius r = 75 cm with $\int B dl = 2.1$ Tm.

- the hadron absorber downstream from the target is made of 60 cm of beryllium oxyde followed by 400 cm of carbon and 80 cm of iron.

The resulting J/ψ mass resolution is 3.1 % (r.m.s) and the acceptance for muon pairs is of the order of 15 % for invariant masses above 3 GeV/c^2.

2.2. The segmented target

The target [4] is made of 7 Pb subtargets located 25 mm apart along the beam axis. Each subtarget is a 1 mm thick disk leading to a total of 17.5 % of an interaction length. Their diameter is 2.5 mm except for the most upstream one which has 5 mm diameter and is thus large enough to intercept 100 % of the incident Pb beam. Each subtarget is followed downstream by two associated quartz blades located off the beam axis. Their Čerenkov light provides the needed vertex identification both for the primary interaction and for any possible further reinteraction of a spectator fragment. The target assembly is "protected" against interactions produced upstream by two "anti-halo" quartz counters located respectively 512 and 187 mm upstream from the central target. They cover an area of 40×40 mm^2 and have a 3 mm diameter central hole to let all the Pb beam pass through, undetected. They are intended to detect multicharged fragments produced by parasitic upstream interactions.

The efficiency of the standard algorithm allowing to identify the subtarget where the inter-

action took place depends only on the multiplicity of the collision. In particular, for a given multiplicity or, equivalently, transverse energy E_T, this efficiency is the same whether the interaction produces a J/ψ or a Drell-Yan muon pair and cancels out in the ratio of the two cross-sections. Nevertheless, as the transverse energy distributions associated with J/ψ and Drell-Yan events are different, the detection efficiencies *averaged* over the whole transverse energy range are different. They are determined and applied separately when computing cross-sections *integrated* over E_T.

When studying separately the sample of the most peripheral events, and only in this case, a target algorithm looser than the standard one is used to identify the interaction subtarget. This allows to increase the statistics of this specific sample of events and thus to study more peripheral collisions.

2.3. The multiplicity detector

The multiplicity detector (MD) is located between the last subtarget and the beryllium oxyde preabsorber. It consists of two identical units, each one with about 7000 silicon microstrips, measuring charged particles in the pseudo-rapidity range $1.5 < \eta < 3.9$. A preliminary description of this device is given in [5]. Due to the incomplete configuration of the MD in the 1995 run, and to the preliminary status of its analysis, it has not been used for the work presented in this paper.

2.4. The BeO preabsorber

The multiplicity detector is followed downstream by a 60 cm long conical preabsorber, made of BeO, which has its front face 25 cm downstream from the target center. It covers the pseudo-rapidity region $2.65 < \eta < 6.20$ and is thus located along the muon paths from the target to

the spectrometer. A central hole along the beam axis allows the ions which have not interacted in the target to pass through on their way to the ZDC and the uranium beam dump.

2.5. The electromagnetic calorimeter

The BeO preabsorber is surrounded by the electromagnetic calorimeter (EC) which measures the transverse neutral energy produced in the interaction. The EC has its front face 32 cm downstream from the target center. It covers a pseudo-rapidity interval $1.1 < \eta < 2.3$, outside the spectrometer acceptance. It is made of 2 mm diameter scintillating fibers embedded in a 14 cm thick lead converter in a 1 : 2 volume ratio ($L_{rad} = 0.93$ cm). Its readout is divided into six sextants and each sextant is subdivided into four sectors allowing measurements in roughly equal pseudo-rapidity bins. Its resolution is 5 % for central Pb-Pb collisions. Contamination due to charged particles contributes to 40 % of the raw transverse energy measured by the electromagnetic calorimeter. This contamination is estimated from a Geant-based simulation and subtracted from the raw measurement in order to provide the neutral transverse energy spectrum which is used in this paper.

2.6. The very forward calorimeter

The very forward calorimeter or "zero-degree" calorimeter (ZDC) measures the energy carried out from the Pb-Pb reaction by the beam spectators. It is located along the beam axis, with its front face 165 cm downstream from the target centre. It is placed within the main carbon muon filter, immediately upstream from the beam dump core of the hadron absorber. In order to stand the huge radiation dose, it is based on the quartz fibre technique [6]. Similarly to the classical "spaghetti" calorimeters, silica optical fibers (365 μm in diameter) are embedded in a tantalum converter with a volume ratio 1 : 17. This converter is 65 cm long and its section normal to

the beam direction is 5×5 cm^2. The calorimeter measures the Čerenkov light produced by beam spectators showering in the tantalum converter. In order to minimize the contamination arising from particles produced in the collision, its angular acceptance is defined by an upstream 60 cm long copper collimator, through a conical hole slightly larger than the beam divergence. Its energy resolution is 7 % for 32.7 TeV incident ^{208}Pb nuclei.

2.7. The beam hodoscope

A beam hodoscope (BH) is used to identify and count the incident ions. It is also used to reject events where two or more incoming ions arrive so close in time, i.e. less than 20 ns[1] apart, that potential piled-up interactions could bias the measurements provided by the detectors in the target region. Finally, the BH signals are also used, after the spectrometer has detected a muon pair candidate, to precisely time the dimuon trigger with less than 1 ns jitter with respect to the Pb-ion time of arrival. The BH is made of a single plane of 16 quartz counters, 0.7 mm thick each. It is located 22 meters upstream from the target, in a region where the beam spot is large enough to reduce individual counting rates. Six auxiliary detectors (BHI) made of scintillator counters are located immediately downstream, off the beam axis. They tag, for off-line rejection, events where the incident Pb-ion has interacted in the BH itself.

3. Data taking conditions

The experiment made use of an incident beam of $3 \, 10^7$ ions per burst on the average, leading to $4.8 \, 10^6$ interactions in the 4.5 s spill. The muon pair trigger provided by the hodoscopes of the spectrometer fired at the rate of 900 events per burst.

During the spill, the data from each detector subset (MD, PC, ZDC,...) are stored into buffer

---

[1]20 ns is the duration of the reading gate of most of the individual subdetectors (12 ns for the ZDC).

memories by means of a network of 24 transputers, providing enough parallelism to stack the information of the whole burst, i.e. up to 5000 events and/or 17 Mbytes. At the end of the spill, the network checks the validity of the data and the result is summarized for each event in a status register. The data of the whole burst and the status are then transferred in parallel via transputer links (20 Mbits/s) to the burst buffers located in the acquisition crate. The same data are simultaneously sent to identical burst buffers in the "spy" crate, shared by 6 microprocessors dedicated to flexible on-line analysis, without interference with the activity in the acquisition crate.

During the interburst, a front end microprocessor reads the event partitions located in the burst buffers in order to build the events, rejects them when a partition mismatch is detected, checks for event integrity and writes on cartridge the good events in the burst. It also transmits the same information to the central computer which controls the whole acquisition system (run types, hardware and software initializations and controls). Data from individual subdetectors are monitored with the help of three dedicated work stations.

More details on the acquisition procedure can be found in [7] and [8]. A total amount of about 60 million events were written on tape during the 1995 run (6 weeks).

4.   Event selection

The muon off-line reconstruction program requires that at least two tracks in the air sectors of the toroidal magnet are reconstructed from the hits in the multiwire proportional chambers and that the corresponding trigger counters have fired. Furthermore, the tracks must have a common origin in the target region. The above reconstruction criteria are satisfied by 45% of the offline processed events. In order to be selected for the final analysis event sample, events

have to satisfy a "general" selection procedure according to the criteria described hereafter:

- One and only one incident ion is detected by the beam hodoscope within the 20 ns gate opened by the trigger. This severe beam condition selects interactions totally free from pile-up at the price of rejecting 20% of the events. It can be dropped without affecting the results as in most of the cases (84%) where two "simultaneous" incoming ions are present, only one of them interacts in the target and in the remaining 3.2% of the total sample, the target algorithm still rejects about half of them.

- Only one incident ion is detected by the ZDC. This selection is based on a shape analysis of the ZDC signal. It is redundant with the previous one when inefficiencies are neglected.

- The target algorithm identifies one and only one subtarget as origin of the interaction. This condition rejects events where two incoming ions have interacted in two different subtargets and events where a projectile spectator reinteracts in a subsequent subtarget.

- The Pb-ion associated with the event has not interacted in the BH or, more generally, somewhere upstream from the target. This selection is based on the information provided by the BHI and anti-halo counters as described above.

- Two and only two tracks satisfy the reconstruction requirements.

The kinematical parameters of the muons are then computed with their common origin assigned to the center of the identified subtarget.

Finally, for background subtraction purposes and as explained below, a fiducial cut is required which guarantees that the acceptance of the spectrometer is independent of the electric charge of the detected muons. This is obtained by rejecting muon pairs where at least one of the muons would be lost from the sample of accepted tracks if it had the opposite charge at the entrance of the magnet.

The above selection criteria lead to a final sample of events which includes about 50 000 J/ψ, and 630 Drell-Yan events with mass higher than 4.2 GeV/c^2.

5. Analysis

The aim of the analysis presented hereafter is to determine the J/ψ and Drell-Yan yields in Pb-Pb interactions. J/ψ mesons are identified through their muon pair decay. A good reference is provided by the Drell-Yan mechanism which also produces opposite sign muon pairs of similar features in the same invariant mass range.

For invariant masses above 2 GeV/c^2, opposite sign pairs originate also from the production and decay into muons of $D\bar{D}$ pairs and ψ' mesons. The main contribution to this sample, however, is due to multiple π and K meson production and decay, called from here on "the background". The π and K decays lead also to like-sign pairs which are used to estimate this background in the sample of opposite sign dimuons. Using a standard procedure[9] which requires, nevertheless, that the probability to detect a muon in the apparatus is independent of its sign and of the sign of the second muon of the pair (hence the "fiducial" cut described above), the number of "signal" events is obtained from the raw number N^{+-} of opposite sign muon pairs after subtraction of the background according to the relation:

$$Signal^{+-} = N^{+-} - 2 \times \sqrt{N^{++} \times N^{--}}$$

where N^{++} (resp. N^{--}) is the number of pairs made of two positive (resp. negative) charged muons.

The analysis is restricted to muon pairs within the kinematical domain where the accep-

9

tance of the spectrometer is sizeable, i.e. above 10% of its maximum. It is thus required for the final sample of events that the dimuon rapidity in the laboratory frame lies in the range $2.92 \leq y_{lab} \leq 3.92$ [1] and that the polar decay angle of the muons in the Collins-Soper reference frame satisfies $\mid \cos \theta_{CS} \mid < 0.5$. Figure 3 shows the invariant mass spectrum for the opposite sign, background and signal muon pairs of the final sample, not corrected for acceptance. The signal to background ratio is larger than 10 at the J/ψ peak. There are roughly 5% non-J/ψ signal events under the J/ψ peak. They are mainly due to Drell-Yan events as the $D\bar{D}$ contribution is expected to be, at a mass of 3 GeV/c^2, one order of magnitude lower.

In order to determine the number of events originating from the J/ψ decay and from the Drell-Yan mechanism, the analysis proceeds as described hereafter.

The mass spectrum above 3.05 GeV/c^2 is fitted to an expression which accounts for the superposition of a continuum and two "pseudo-gaussian" functions which reproduce with good accuracy the resolution of the detector as determined by Monte-Carlo simulations. The lower bound of the fitted spectrum is chosen in order to reduce unknown contributions [10] and minimize background subtraction systematics.

Apart from the background, the dominant contribution to the continuum is due to the Drell-Yan events, parametrized as the sum of two exponential functions:

$$dN/dM \propto [\, \exp\left(-P_1 M\right) - P_2 \times \exp\left(-P_3 M\right)\,]$$

with the parameters P_i deduced from a fit to Monte-Carlo generated Drell-Yan events after simulated detection, reconstruction and selection.

---

[1] In the cms reference frame, the corresponding condition is $0 \leq y_{cms} \leq 1$.

The shape of the tail of the $D\bar{D}$ contribution is likewise parametrized as:

$$dN/dM \propto [\exp(-C_1 M) - C_2 \times \exp(-C_3(M - C_4)^3)]$$

from a fit to Monte-Carlo generated $D\bar{D}$ events. The ratio of the $D\bar{D}$ to Drell-Yan events is fixed from the study of the dimuon mass spectrum in p-W collisions at 200 GeV/c [10].

The mass shape of the reconstructed J/ψ resonance is well described by:

$$dN/dM \propto \exp((M - \mu)^2/2\sigma_0^2\, f(M))$$

with $f(M)$ determined by simulation. A similar shape is taken for the ψ' resonance. More details on the Monte-Carlo procedures can be found in [11].

The final fit to the signal mass spectrum uses the maximum likelihood method to determine the number of events of the different contributions, i.e. N_{DY}, $N_{J/\psi}$ and $N_{\psi'}$. For a better quality fit to the data, the J/ψ parameters μ and σ_0 are left free. The corresponding parameters for the ψ', i.e. μ' and σ_0', are related to μ and σ_0 according to the nominal mass difference and simulated width ratio. The best fit to the data provides a $\chi^2/\text{dof} = 0.99$.

6. Absolute cross-sections

Absolute cross-sections are computed taking into account the incident Pb-ion flux given by the BH detector. The beam spot size[1] is small enough so that after precise steering on the

---

[1] Depending on the two different optics which were used during the run, the horizontal and vertical beam spot sizes were respectively $\sigma_x = 0.5\ mm$, $\sigma_y = 0.5\ mm$ and $\sigma_x = 0.35\ mm$, $\sigma_y = 0.45\ mm$. With the first optics, the small subtargets intercepted only 75 % of the beam.

center of the targets monitored by the trigger rate itself, 100% of the beam intercepts the first (large) target. Targetting efficiency on the subsequent (small) subtargets is obtained from the ratio of events produced relative to those originating from the first target.

The absolute numbers of events, corrected for detector inefficiencies, selection cut losses and acceptances as detailed in Table 1 lead, in the kinematical domain $\mathcal{D}$ defined by:

$$0 \leq y_{cms} \leq 1 \qquad \text{and} \qquad |\cos \theta_{CS}| < 0.5$$

to the following cross-sections:

$$B_{\mu\mu}\sigma_{J/\psi} \;=\; 21.9 \pm 0.2 \pm 1.6 \;\mu\text{b}$$

$$\text{and}$$

$$\sigma_{DY} \;=\; 1.49 \pm 0.02 \pm 0.11 \;\mu\text{b}$$

in the mass range [2.9 - 8.0] GeV/c^2. The lower limit of this range has been chosen for comparison purpose with other existing results.

The systematic error of 7% results from the uncertainties in the corrections given in Table 1. It includes also a contribution of $\pm 1.5\%$ arising from the change in cross-section occurring when the ratio open-charm to Drell-Yan varies from the value extrapolated from p-W data to the value obtained from the Pb data themselves [10]. In order to reduce sources of systematic uncertainties, the same cross-sections have been computed making use of muon pairs originating only from the first target. The corresponding results agree, within errors, with the values obtained for the whole sample of events.

The data have also been analyzed in the mass range $M_{\mu\mu} > 2.7$ GeV/c^2. The detailed procedure can be found in [4]. Although less insensitive to systematic effects, the results completely

agree with the values reported in this paper within the 1.5% systematic error due to the uncertainty in the description of the mass continuum below the J/ψ peak.

7. Ratio of the J/ψ to the Drell-Yan cross-section as a function of centrality

In order to further investigate the J/ψ cross-section in Pb-Pb interactions, the behaviour of the J/ψ yield is studied hereafter as a function of the centrality of the collision. The impact parameter of the reaction can be experimentally estimated on an event by event basis from the neutral transverse energy or from the energy carried by the projectile spectators, as measured respectively by the electromagnetic and ZDC calorimeters. Figure 4 displays the $E_T - b$ correlation computed using an upgraded version of the method presented in [12]. The strong correlation between the measured value of E_T and the impact parameter of the collision is experimentally confirmed, as shown in figure 5, by the observed correlation between E_T and the energy measured by the ZDC, more directly related to the impact parameter b.

Figure 6 shows the distribution of the measured transverse energy E_T, associated with Drell-Yan muon pairs of invariant mass higher than 4.0 GeV/c^2. The fall of the spectrum in the low E_T region, which corresponds to the most peripheral collisions, is due to the muon pair trigger and to the requirement of subtarget identification, both favouring central collisions. The E_T distribution after correction for the latter effect is also shown in figure 6.

The events of the whole Pb-Pb sample are subdivided into 5 subsamples according to the transverse energy of the interaction. An identical fit procedure as used for the whole sample of events is then applied to each of the five mass spectra. We are thus led to the numbers of events given in table 2 from which we can deduce the corresponding cross-sections.

From these values, we can extract the ratio of cross-sections $\sigma_{J/\psi}/\sigma_{DY}$, as a function of E_T.

Experimentally, this ratio has the advantage of being free from most systematic errors, and in particular the detector inefficiencies and flux uncertainties. These systematic effects are identical for the two samples of events and thus cancel in the ratio.

The values obtained are listed in table 3 and plotted in figure 7 as a function of E_T. The Drell-Yan cross-sections are taken in the mass interval 2.9-4.5 GeV/c^2. To the quoted statistical errors on $\sigma_{J/\psi}$ / σ_{DY} should be added a 1.5% *global* systematic uncertainty arising from the difficulty in describing the lower mass continuum of the Pb data as a trivial superposition of Drell-Yan and open charm contributions (see [10]).

The J/ψ to Drell-Yan cross-section ratio has also been measured for the full sample of events, whatever the centrality. The result is:

$$B_{\mu\mu}\,\sigma_{J/\psi}\ /\ \sigma_{DY} = 16.1 \pm 0.3 \pm 0.2$$

8. Conclusion

In summary, we have measured J/ψ and Drell-Yan production cross-sections in Pb-Pb inter-actions at $\sqrt{s} = 17.4$ GeV. The ratio of the J/ψ cross-section to the Drell-Yan cross-section decreases significantly with decreasing impact parameter. From peripheral to central collisions, J/ψ production is suppressed by a factor of 2 with respect to Drell-Yan. These results are compared in the following letter of this issue [13] with measurements obtained previously with lighter incident ions.

Acknowledgements

14

able in 1995 to deliver Pb ions at 158 GeV/c per nucleon with very high efficiency and an invisible spill time structure. We are deeply indebted to many people of the SL division for their extremely efficient technical assistance in the experimental area. We also thank the technical teams of our home institutes for their support in the construction or in the upgrade of the various detectors of our apparatus.

References

[1] L. Fredj, Thesis, Université Blaise Pascal, Clermont-Ferrand (1991);
    C. Baglin *et al.*, Phys. Lett. B 255 (1991) 459;
    C. Baglin *et al.*, Phys. Lett. B 270 (1991) 105;
    C. Lourenço *et al.*, Quark Matter '93, Nucl. Phys. A 566 (1994) 77c;
    A. Borhani, Thesis, Université Pierre et Marie Curie, Paris (1996).
[2] C. Baglin *et al.*, Phys. Lett. B 220 (1989) 471.
[3] M.C. Abreu *et al.*, Phys. Lett. B 368 (1996) 230;
    M.C. Abreu *et al.*, Phys. Lett. B 368 (1996) 239.
[4] F. Bellaiche *et al.*, LYCEN 97-07, submitted to Nucl. Instr. and Meth.;
    F.Bellaiche, Thesis, Université Claude Bernard, Lyon (1997).
[5] B. Alessandro *et al.*, Nucl. Instr. and Meth. A 360 (1995) 189 and Nucl. Phys. B 44 (1995) 303.
[6] E. Chiavassa *et al.*, Proceedings of the 6th Int. Conf. on Calorimetry in High Energy Physics, Frascati, (1996), 289.
[7] V. Capony, Thesis, Université de Savoie, Annecy (1996).
[8] S. Silva, Thesis, Universidade Técnica de Lisboa, Lisbon (1997).
[9] S. Papillon, Thesis, Université Denis Diderot, Paris (1991), IPNO-T9103.
[10] E. Scomparin *et al.*, Quark Matter '96, Nucl. Phys. A 610 (1996) 331c.
[11] F. Fleuret, Thesis, Ecole Polytechnique, Palaiseau (1997).
[12] C. Baglin *et al.*, Phys. Lett. B 251 (1990) 472.
[13] See the following letter of this issue.

$J/\psi\ (DY)\ target\ identification$	:	$85\ (86) \pm 3$
$Muon\ pair\ trigger$	:	92 ± 5
$Track\ reconstruction$	:	95 ± 2
$Targetting$	:	75 ± 2
	or	$100 + 0 - 2$
$Lifetime$	:	96 ± 1

$Pile - up\ cut\ loss$	:	20 ± 1
$Reinteraction\ cut\ loss$	:	2 ± 1
$BHI\ cut\ loss$	:	2 ± 0.5
$Anti - halo\ cut\ loss$	:	3 ± 1

$Drell\ Yan\ acceptance$		
$(2.9\ \text{GeV}/c^2\ < M_{\mu\mu} <\ 8.0\ \text{GeV}/c^2)$	:	15.4
$(2.9\ \text{GeV}/c^2\ < M_{\mu\mu} <\ 4.5\ \text{GeV}/c^2)$	:	15.2
$J/\psi\ acceptance$	:	13.5

Table 1

Detector efficiencies, selection cut losses and acceptances. All numbers are in %.

E_T bin range (GeV)	$\bar{E}_T$ (GeV)	$\bar{b}$ (fm)	J/ψ	$D - Y$
$5 - 45$	34	9.2	6083	268
$45 - 70$	58	7.7	10273	620
$70 - 105$	88	5.9	16561	1035
$105 - 135$	120	3.9	12278	984
$135 - 175$	147	2.0	8201	726
All E_T	94		53396	3633

Table 2

Number of events as a function of centrality obtained from the fit to the mass spectrum. The numbers of Drell-Yan events are given in the mass interval 2.9-4.5 GeV/c^2. The values of $\bar{E}_T$ and $\bar{b}$ correspond to the average of E_T and b for the events observed in each bin.

E_T bin range (GeV)	$B_{\mu\mu}\sigma_{J/\psi} \ / \ \sigma_{DY}$
$5 - 45$	$25.6 \pm 2.1 \pm 0.3$
$45 - 70$	$18.7 \pm 0.9 \pm 0.3$
$70 - 105$	$18.0 \pm 0.4 \pm 0.2$
$105 - 135$	$14.1 \pm 0.4 \pm 0.2$
$135 - 175$	$12.7 \pm 0.5 \pm 0.2$
All E_T	$16.1 \pm 0.3 \pm 0.2$

Table 3

The ratio of the J/ψ to the Drell-Yan cross-section as a function of centrality. The Drell-Yan cross-sections are taken in the mass interval 2.9-4.5 GeV/c^2. In the last line presenting the results averaged over E_T, the values were corrected to take into account the subtarget identification inefficiency.
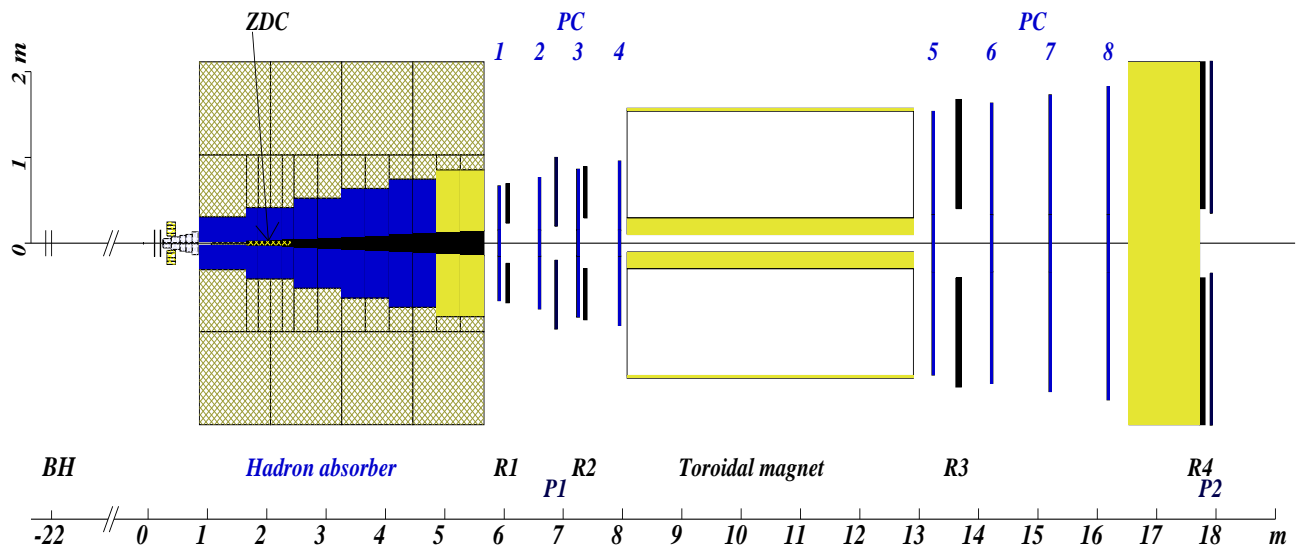
Fig. 1. The NA50 apparatus. Details of the target area are shown in figure 2.
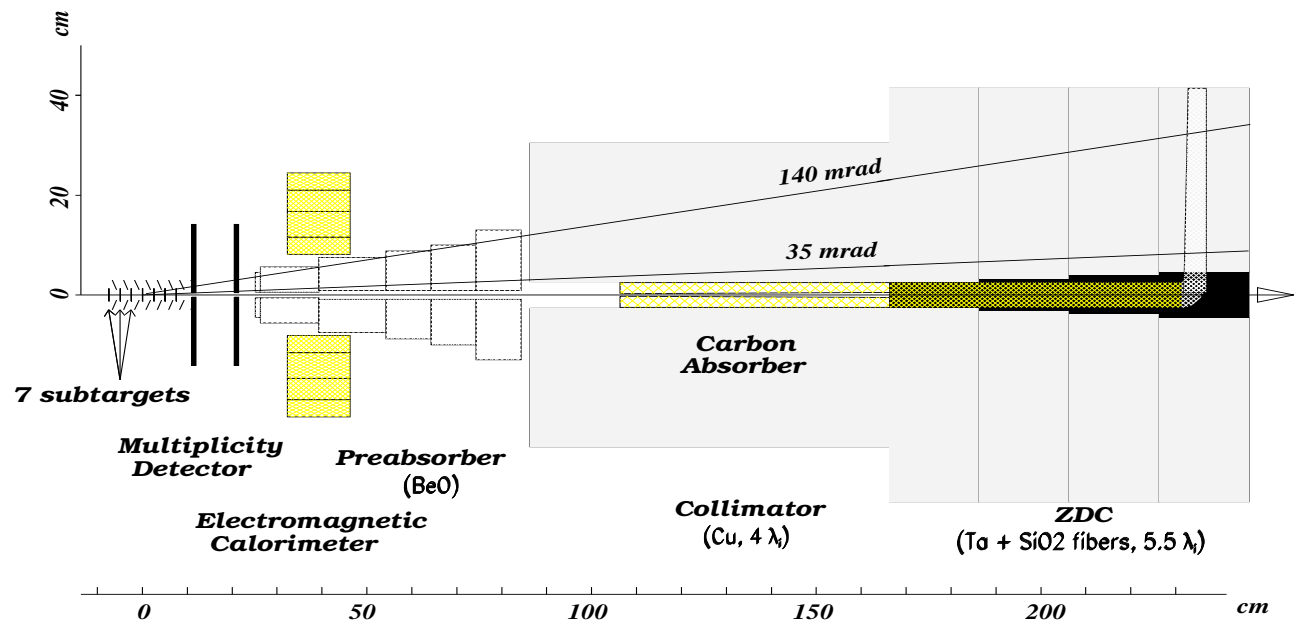
Fig. 2. Lay-out of the various elements of the NA50 detector in the target area.
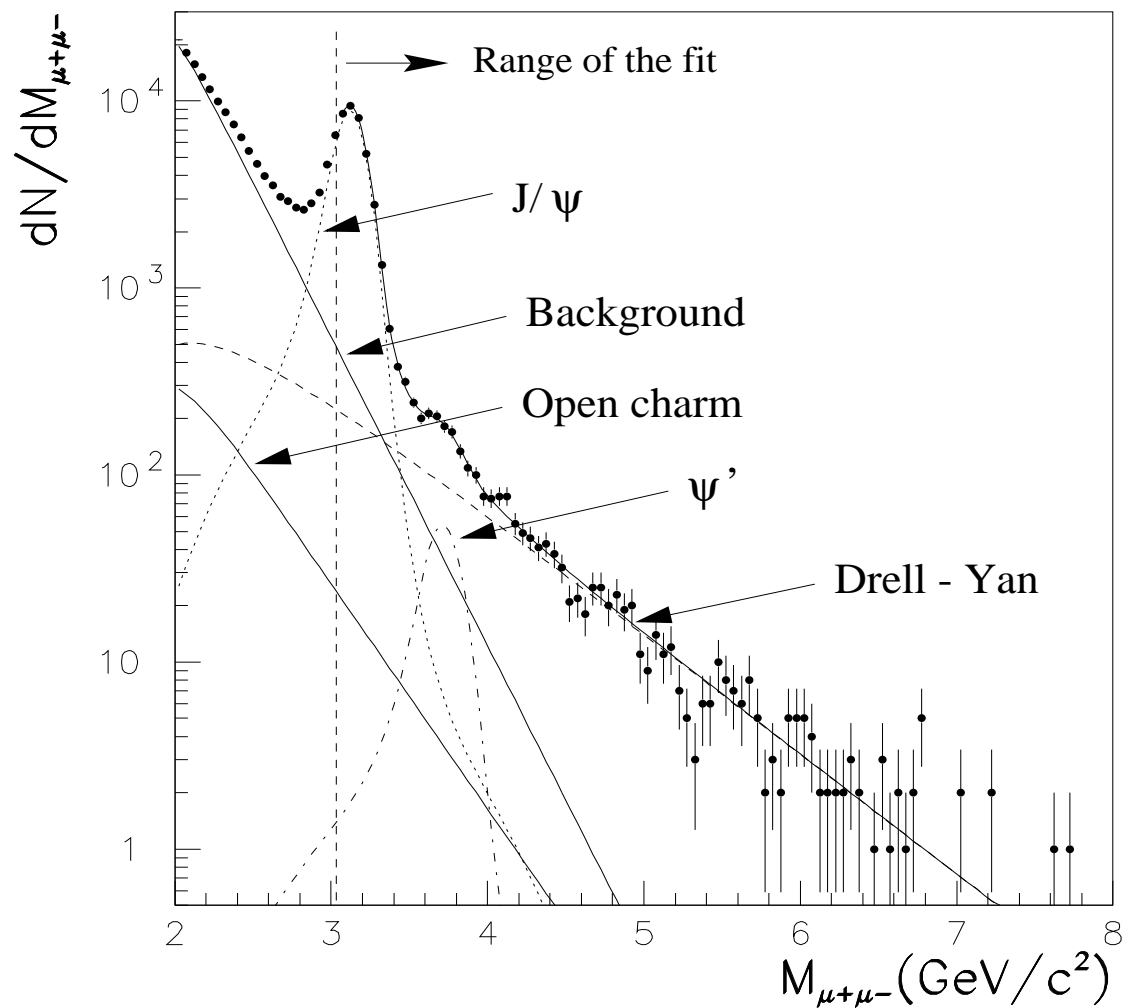
Fig. 3. Muon pair invariant mass spectrum for Pb-Pb collisions at 158 GeV/c incident momentum.
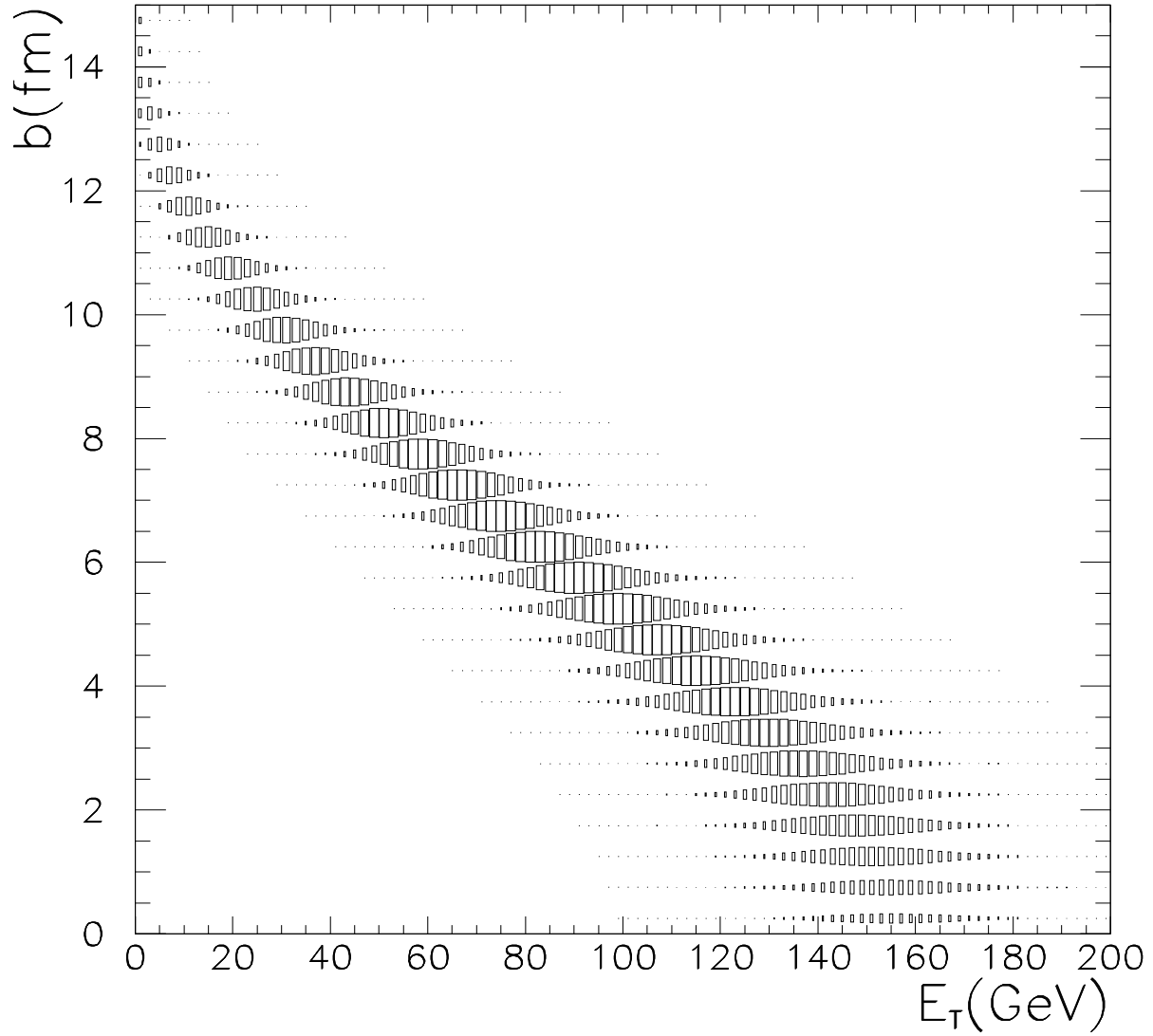
Fig. 4. Correlation between the transverse energy E_T and the impact parameter b calculated for Pb-Pb collisions at 158 GeV/c for Drell-Yan events.
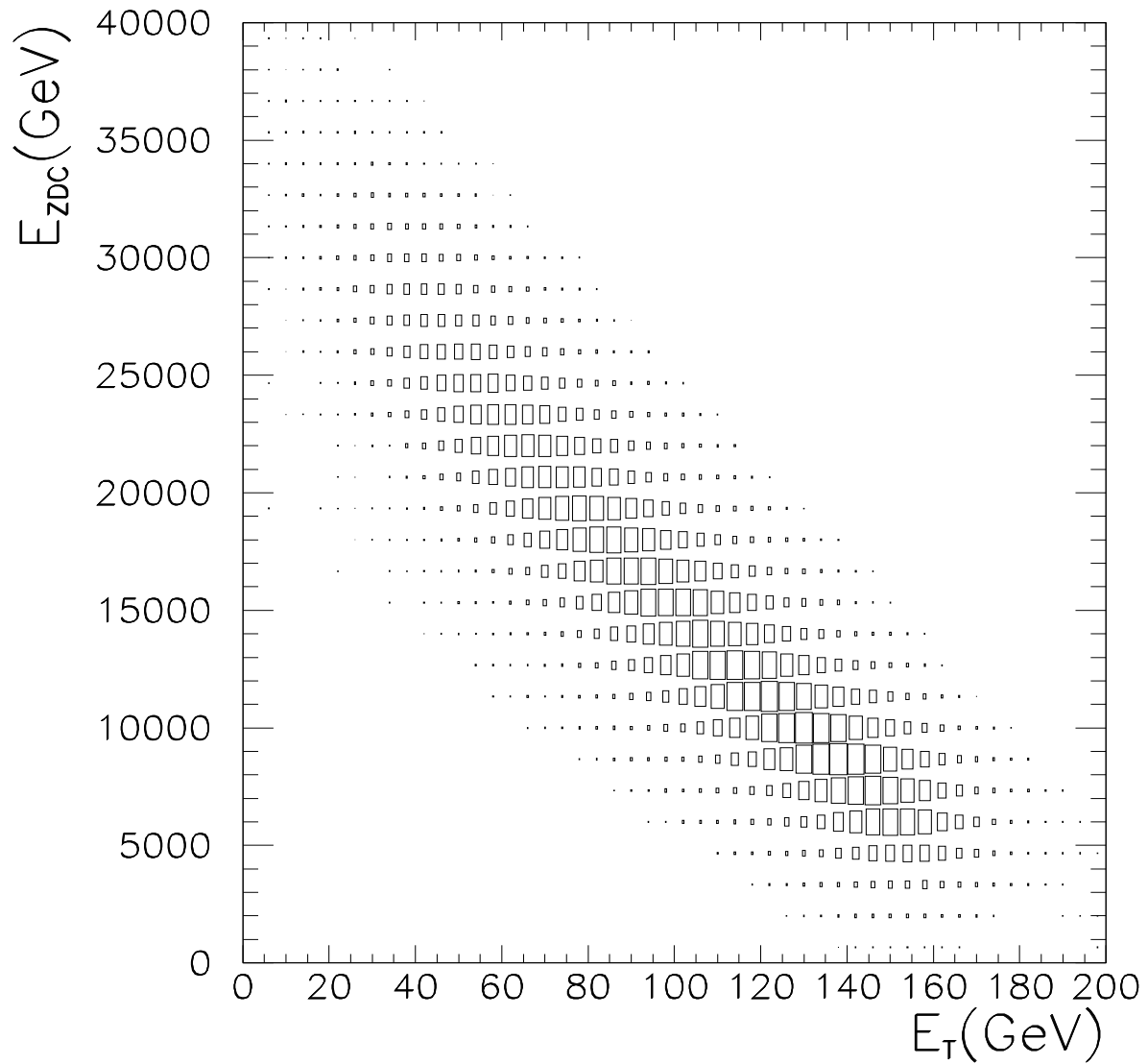
Fig. 5. Observed correlation between the neutral transverse energy measured in the electromagnetic calorimeter and the forward energy measured by the "zero degree calorimeter". The data correspond to dimuon events with $M_{\mu\mu} > 2.0 \text{ GeV}/c^2$, not corrected for subtarget identification efficiency.
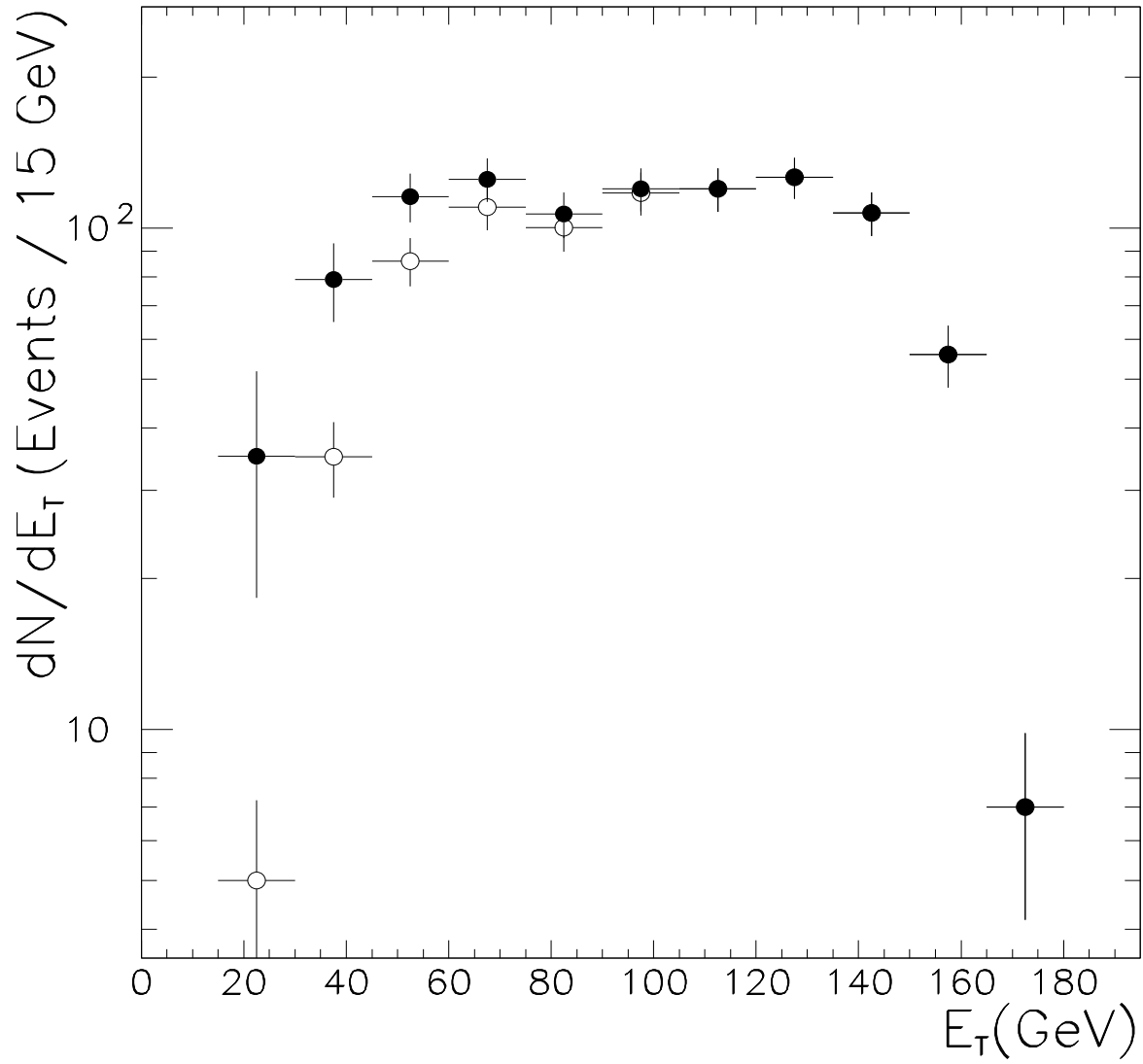
Fig. 6. Neutral transverse energy spectrum of Drell-Yan muon pairs with mass larger than 4.0 GeV/c^2, before (open circles) and after (closed circles) correction for the subtarget identification efficiency.
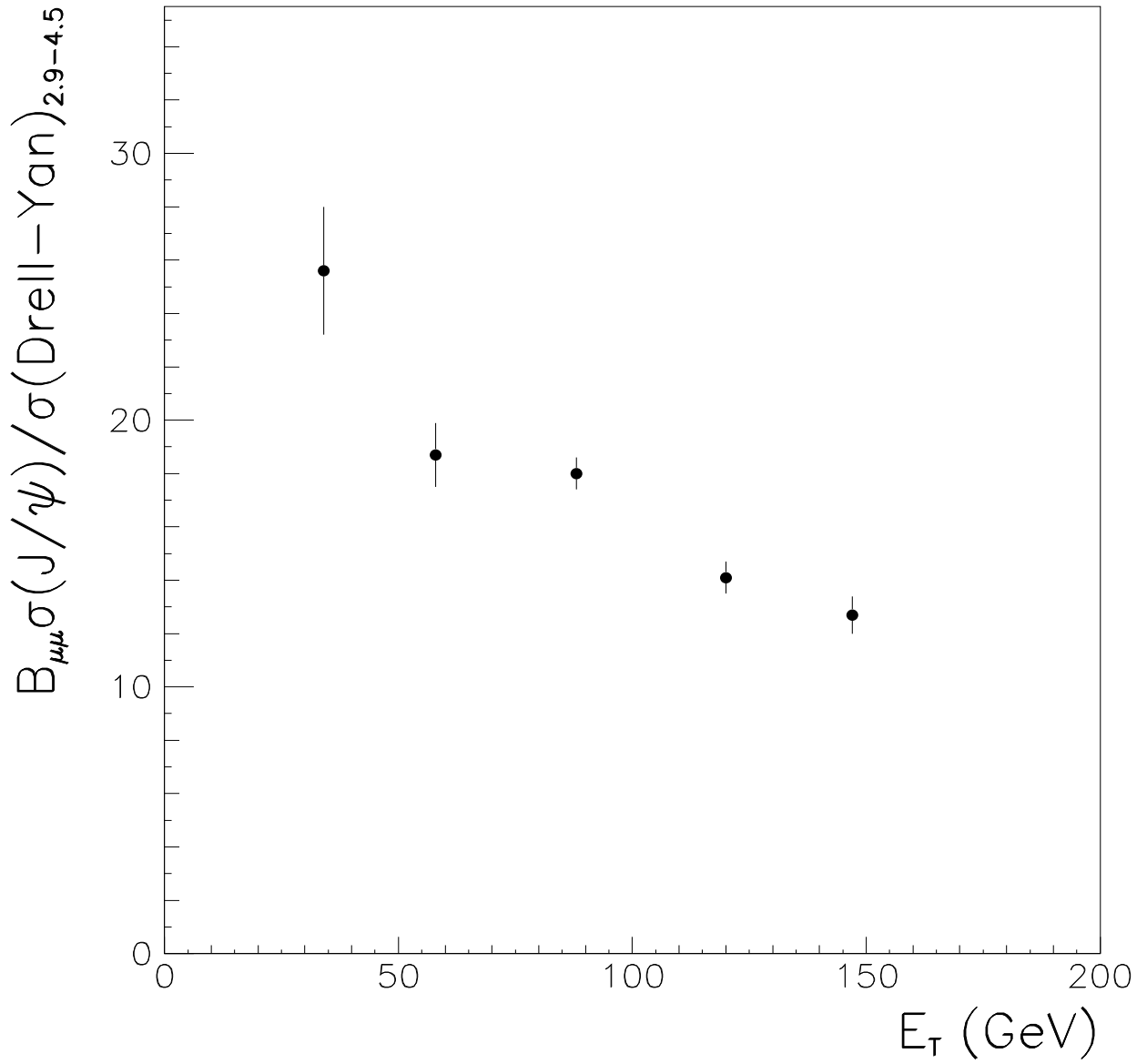
Fig. 7. The ratio of J/ψ to Drell-Yan cross-sections as a function of E_T. The Drell-Yan cross-sections are taken in the mass range $2.9 - 4.5$ GeV/c^2.